M. Romero, J. Ma. Rincón, S. Mûsik and V. Kozhukharov, Mössbauer effect and X-ray distribution function analysis in complex Na_2O-CaO-ZnO-Fe_2O_3-Al_2O_3-SiO_2 glasses and glass-ceramics
Materials Research Bulletin 34 (1999) 1107-1115; DOI: 10.1016/S0025-5408(99)00110-5

MÖSSBAUER EFFECT AND X-RAY DISTRIBUTION FUNCTION ANALYSIS IN COMPLEX Na_2O-CaO-ZnO-Fe_2O_3-Al_2O_3-SiO_2 GLASSES AND GLASS-CERAMICS

Maximina Romero[1*], Jesús. Ma. Rincón[1], Svetozar Mûsik[2], Vladimir Kozhukharov[3]

[1]Glass-Ceramic Lab., Instituto E. Torroja de Ciencias de la Construcción (CSIC), C/ Serrano Galvache s/n, 28033 Madrid, Spain

[2]Ruder Boskovic Institute. P.O. Box 1016, 10001 Zagreb, Croat

[3]Higher Institute of Technology. University of Sofia. Kl. Okhridski, 1756 Sofia, Bulgary

ABSTRACT

Mössbauer spectroscopy at room temperature has been carried out to determine the state of iron ions in complex glasses and glass ceramics in the SiO_2-CaO-ZnO-Na_2O-Fe_2O_3-Al_2O_3 system. Isomer shift values of the glasses suggest that Fe^{3+} and Fe^{2+} are in tetrahedral and octahedral coordination respectively. The spectrum of the glass-ceramic shows that about 60 wt % of total iron is in the magnetite phase. The Fe^{+3}/Fe^{+2} ratio varies with the total iron oxide content of the glasses indicating that the vitreous network is more distorted when the iron content is greater. X-ray diffraction measurements have been carried out to obtain the radial distribution function (RDF). The interatomic distances for Si-Si and Si-O have been determined. The complex composition of these glasses does not allow the estimation of Al-O and Fe-O distances.

KEYWORDS: A. glasses, A. ceramics, C. Mössbauer spectroscopy, C. X-ray diffraction

1. INTRODUCTION

Mössbauer spectroscopy is a nuclear resonance technique widely applied on the study of glasses containing iron oxide (1). Measurement of isomer shift (IS) and quadrupole splitting (QS) values allows the determination of oxidation state and coordination of iron ions in glasses. Kurkjian et al. (2) applied the Mössbauer spectroscopy on silicate and phosphate glasses and concluded that Fe^{3+} ions change from octahedral to tetrahedral sites when the P_2O_5 content in the glass increase. Gosselin et al. (3) found Fe^{3+} in octahedral sites in sodium trisilicate glasses. According to these authors, the Fe^{2+}/Fe^{3+} ratio decreases when the total iron oxide content in the

* Corresponding author, e-mail address: mromero@ietcc.csic.es

glass increases. Tarangin et al. (4) obtained the same result in borosilicate glasses with iron oxide content in the 1.5 - 8.1 wt % range. Labar et al. (5) suggest the interpretation of this fact on the basis of the greater stability of Fe^{3+} cations due to both the ionic radii and the glass dielectric constant. The Mössbauer effects on glasses in the SiO_2-CaO-Fe_2O_3-Al_2O_3 and SiO_2-Na_2O-Fe_2O_3-Al_2O_3 systems have been reported by Pergamin et al. (6) Fe^{3+} ions are located in tetrahedral and octahedral sites in glasses containing CaO. However, when the glass contains Na_2O, $Fe3^+$ ions are located only in tetrahedral sites.

Hirao et al. (7) studied the changes of Mössbauer parameters when glasses in the Na_2O-Fe_2O_3-SiO_2 system are subjected to heat treatment, using iron silicate compounds having known coordination as references. The change in IS indicates that Fe^{3+} ions are located in tetrahedral sites in glasses with high iron oxide content and prefer octahedral state when the iron oxide content in the glass is lower. They found no changes in QS when the glass composition varies but the QS value is lower after heat treatment of glass.

The aim of this work is to study by Mössbauer spectroscopy the oxidation and coordination states of iron in some complex glasses and glass-ceramic in the SiO_2-CaO-ZnO-Na_2O-Fe_2O_3-Al_2O_3 system. The structural characterization of these glasses and glass-ceramic by means of X-ray distribution function analysis is also presented.

2. EXPERIMENTAL METHODS

Goethite mud (FeOOH), dolomite ($CaCO_3$.$MgCO_3$) and glass cullet were used as raw materials for the preparation of the glasses (G4, G5 and G9) and glass-ceramic (G1). The feasibility of using these raw materials in glass production has been reported in previous works (8). The compositions studied in this work are shown in Figure 1.

The raw materials were weighed precisely to form a given composition and mixed in a ball mill for 10 min. 30 g of mixture were placed in fireclay crucible and melted in air at 1450°C. A hold time of 30 minutes was used to promote homogenization. After melting, the melts were casted on a copper plate. An annealed step at 500°C for 2 hours was performed to avoid mechanical stresses. The glass-ceramic was produced following a petrurgical way. After casting the melt

was cooled down in air. The high iron oxide content of the melt composition allows the crystallization of magnetite crystals during the cooling.

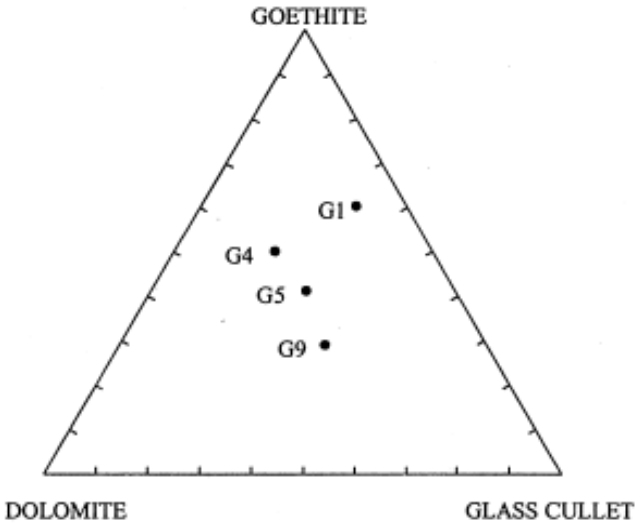

Figure 1. Composition of the glasses (G4, G5 and G9) and glass-ceramic (G1).

X-ray diffraction analyses to study the amorphous or crystalline nature of the studied glasses and glass-ceramics have been reported in a former work (9).

^{57}Fe Mössbauer spectra were recorded in transmission mode at room temperature using a constant velocity drive operating in conjunction with a 250 channel analyzer. The source matrix was ^{57}Co/Rh and the absorbed was prepared by spreading the powdered glass or glass-ceramic over a 1cm diameter disc. Equipment calibration using standard iron foil was carried out after every test. The obtained Mössbauer spectra were analyzed by least-squares fitting of symmetrical, Lorentzian-shaped sextets and doublets to the experimental data.

X-ray diffraction by amorphous dispersion was accomplished in a Philiphs PW 3710 X-ray diffractometer using MoK_α radiation in the wave-vector range of Q = 5-115 nm^{-1}. Here $Q = 4\pi \sin\theta / \lambda$, where θ is half the angle between the incident and diffracted beams, and λ is the wavelength of the incident beam. After applying corrections for absorption, polarization, and Compton scattering (10, 11) to the measured intensity data, the X-ray scattering intensities were converted into electron units, by the generalized Krogh-Moe-Norman method (12), and then the reduced interference function Qi(Q) was obtained, which is defined as

$$i(Q) = \frac{I_{eu}(Q) / N - \sum_{uc} f_j^2}{f_e^2} \qquad [1]$$

where I_{eu}/N is the intensity of the unmodified scattering and f_j and f_e are the atomic scattering factor and the average scattering factor per electron, respectively.

The electron radial distribution function (RDF) can be estimated by applying Fourier transformation to Qi(Q)

$$RDF_{exp} = 2\pi^2 r\rho_e \sum_{uc} Z_j + \int_0^{Q_{max}} Qi(Q) \exp\ (-\alpha^2 Q^2)\ \text{sinQr dQ} \qquad [2]$$

where ρ_e is the average number density of electron and Z_j is the atomic number of the j element. The term of $[-\alpha^2 Q^2]$ is a convergence factor, usually introduced to minimize the truncation error and weigh down the uncertainties at the higher wave-vector region. However, the value of α is assumed to be zero in the calculation of the experimental RDF. In the present work, a RDA program was used for data treatment, calculation of structural factors and determination of radial distribution (13). Radial distribution curve provides information about short range order (SRO) due to bonds between tetrahedron [SiO_4] and about intermediate range order (IRO) due to ordered regions from the vitreous network. From the maximum peak positions, it is possible to know the distances to the reference atom, while the areas of the maximum peaks are related with the number of atoms surrounding to a reference atom. In the glasses studied in this work, which belong to the SiO_2-CaO-ZnO-Na_2O-Fe_2O_3-Al_2O_3 system, the radial distribution function will give information of the Si-O, O-O, Si-Ca, Si-Zn, Al-O, Fe-O, and other pairs.

3. RESULTS AND DISCUSSION

The chemical composition of the glasses and glass-ceramic determined by X-ray fluorescence analysis is shown in Table 1.

Figure 2 shows the Mössbauer spectra obtained from G5 and G9 glasses and G1 glass-ceramic. The glasses have absorption bands in the central part of the spectrum. In G1 glass-ceramic magnetic bands corresponding to magnetite phase are also observed. Mössbauer parameters obtained from the deconvolution of the bands are shown in Table 2. Oxidation state and

coordination of iron atoms in the vitreous network and the percentage of iron in each oxidation state, calculated from Mössbauer parameters are presented in Table 3 (14).

Table 1. Chemical composition (wt %) determined by X-ray fluorescence analysis for G1 glass-ceramic, G4, G5 and G9 glasses.

	G1	G4	G5	G9
SiO_2	38.41	39.46	42.68	44.90
Al_2O_3	6.42	10.80	8.04	3.63
Fe_2O_3	29.24	23.39	20.53	18.04
CaO	6.63	9.46	11.24	13.99
MgO	2.85	4.63	5.37	6.58
ZnO	9.47	7.02	6.15	5.27
PbO	2.24	1.73	1.52	1.32
Na_2O	3.92	2.54	3.61	5.68
K_2O	0.81	0.98	0.86	0.60

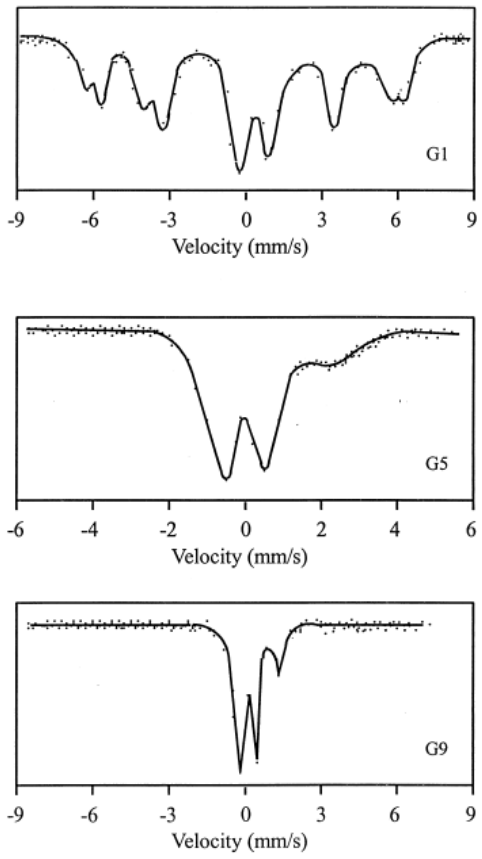

Figure 2. Mössbauer spectra obtained from G5 and G9 glasses and G1 glass-ceramic.

Table 2. Mössbauer parameters obtained from G1 glass-ceramic, G5 and G9 glasses.

	DECONVOLUTION		δ (mm/s)	Δ (mm/s)
G1	2 sextets + 2 doublets	S1	0,28	0,05
		S2	0,50	0,07
		D1	1,09	2,34
		D2	0,49	1,67
G5	4 doublets	D1	0,15	1,51
		D2	0,99	2,12
		D3	0,83	1,51
		D4	0,15	0,92
G9	2 doublets	D1	0,16	1,09
		D2	0,97	2,06

δ = Isomer shift; Δ = Quadrupole splitting

Table 3. Oxidation state, coordination state, iron content and Fe^{3+}/Fe^{2+} calculated from Mössbauer parameters for G1 glass-ceramic, G5 and G9 glasses.

	DECONVOLUTION	**OXIDATION STATE**	**COORDINATION**	**PERCENTAGE**	**Fe^{3+}/Fe^{2+}**
G1	S1	Fe_3O_4	---	17,0	2,6
	S2	Fe_3O_4	---	41,4	
	D1	Fe^{2+}	octahedral	11,4	
	D2	Fe^{3+}	tetrahedral	30,2	
G5	D1	Fe^{3+}	tetrahedral	28,0	4,9
	D2	Fe^{2+}	octahedral	12,6	
	D3	Fe^{2+}	octahedral	4,1	
	D4	Fe^{3+}	tetrahedral	55,3	
G9	D1	Fe^{3+}	tetrahedral	84,3	5,3
	D2	Fe^{2+}	octahedral	15,7	

In G5 and G9 glasses, 100 wt % of iron ions is present in the vitreous network. In G1 glass-ceramic two sextets corresponding to the magnetite phase indicate that 58,5 wt % of the iron is in this crystalline phase. Iron atoms, which are in the vitreous network, have Fe^{2+} and Fe^{3+} oxidation states. The coordination of Fe^{3+} ions is found to be tetrahedral, which is in good agreement with results obtained by others authors (15, 16). Indeed, theses authors have shown that Fe^{3+} ions occupy tetrahedral coordination in the vitreous network when $Fe^{3+}/Fe^{2+}>1$. In G1 glass-ceramic and G9 glass all the Fe^{2+} ions are present in octahedral coordination. In G1 glass-ceramic the isomer shift associated to Fe^{2+} ions in octahedral sites shows a value of 0.50 mm/s. This value is smaller than the value usually found for Fe^{2+} ions in octahedral sites in magnetite (0.67 mm/s) (17). Because G1 glass-ceramic contains Ca^{2+}, Zn^{2+}, Al^{3+} and Si^{4+}, it is likely that these cations are substituted for Fe^{3+} and Fe^{2+} ($Fe^{2.5+}$) in their normal sites. This substitution affects magnetic properties as well as lattice parameter of magnetite. Consequently, the Mössbauer spectrum is also influenced by this possible substitution. The D3 doublet from G5 glass has isomeric shift and quadrupole splitting values nearly to Fe^{2+} in tetrahedral coordination (δ=0,9-1 mm/s and Δ= 1,4-2 mm/s). Since there are no data about this coordination for Fe^{2+} ions in oxidant atmosphere melted silicate glasses, the D3 doublet from G5 glass should correspond to a deformed octahedral position (18).

The quadrupole splitting value varies from 1.67 mm/s (G1 glass-ceramic) to 1.09 mm/s (G9 glass) for Fe^{3+} ions and from 2.34 mm/s (G1 glass-ceramic) to 2.06 mm/s (G9 glass) for Fe^{2+} ions. This decreasing in quadrupole splitting values for both Fe^{3+} and Fe^{2+} ions indicates that network positions occupied by Fe ions have less symmetry and are more distorted when iron oxide content is greater.

Finally, the Fe^{3+}/Fe^{2+} ratio is found to increases from G1 glass-ceramic to G9 glass when the iron oxide content decreases. The Fe^{3+}/Fe^{2+} ratio is influenced by many parameters such as glass composition, melting temperature, cooling rate, furnace atmosphere, etc. As the same melting conditions have been used to prepare G1 glass-ceramic, G5 and G9 glasses, the variation in the glass composition could only be attributed to the decrease in the Fe^{3+}/Fe^{2+} ratio (19). Due to the different contents in iron oxide, the thermal conductivity of these glasses must be different. Variations in heat dissipation after cooling could also affect to the final Fe^{3+}/Fe^{2+} ratio.

Figure 3 shows the X-ray diffraction profiles of the G4, G5 and G9 glasses. An important dispersion takes place in 2θ = 10-40° interval (SRO) followed by a decrease in the X-ray

dispersion from 40° to 80° (IRO). The basic features of these diffraction profiles are similar to those of typical oxide glasses.

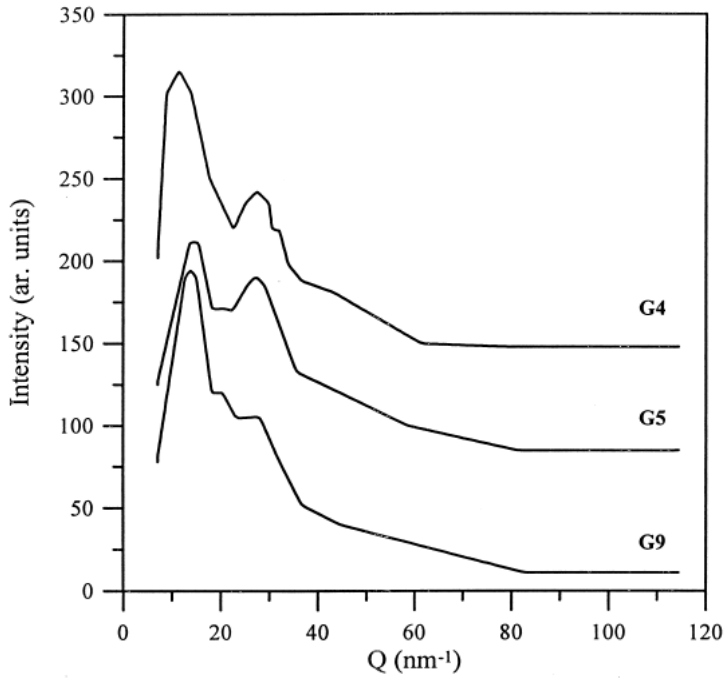

Figure 3. X-ray diffraction profiles for G4, G5 and G9 glasses.

Figure 4 shows the reduced interference functions Qi(Q). The first peak appears about Q = 20 nm^{-1} followed of a considerable number of peaks in all Q range. The existence of these peaks suggests the existence of local ordering. The RDFs of the glasses, which is obtained by the Fourier transformation of the Qi(Q) function, are shown in Figure 5. G4 glass shows a IRO greater than G5 and G9 glasses. G4 glass shows higher percentage of iron oxide than G5 and G9 glasses, which has a large influence in the nucleation and crystallization of silicate glasses (20). The high percentage of iron oxide in G4 glass likely is originating the differences observed in the degree of intermediate range order due to the formation of ordered regions comprised by small nuclei. G4 glass also shows more complexity in SRO. The first peak appears about 0.16 nm being identified with Si-O contribution. In G4 glass a shoulder at 0.21 nm correspond to Al-O and Fe-O pairs. The second important peak about 0.32 nm is related with Si-Si contribution. The O-O pair is only identified in G9 with a small peak at 0.27 nm. Finally, the band at 0.45 nm corresponds to the mixed contribution of several pairs such as Fe-O for Fe^{2+} in octahedral coordination, Zn-O or Pb-O in octahedral coordination and non-bridging O-O.

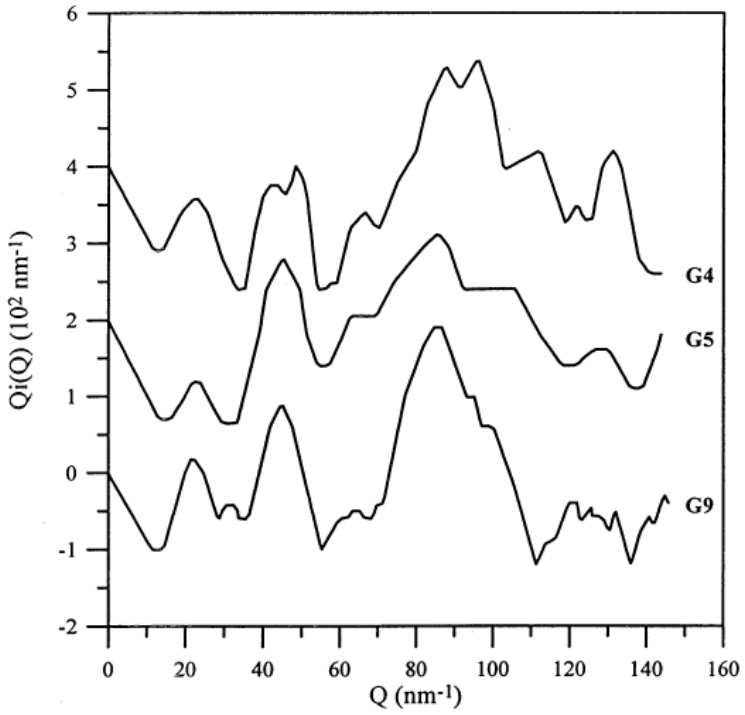

Figure 4. Reduced interference function of Qi(Q) for G4, G5 and G9 glasses.

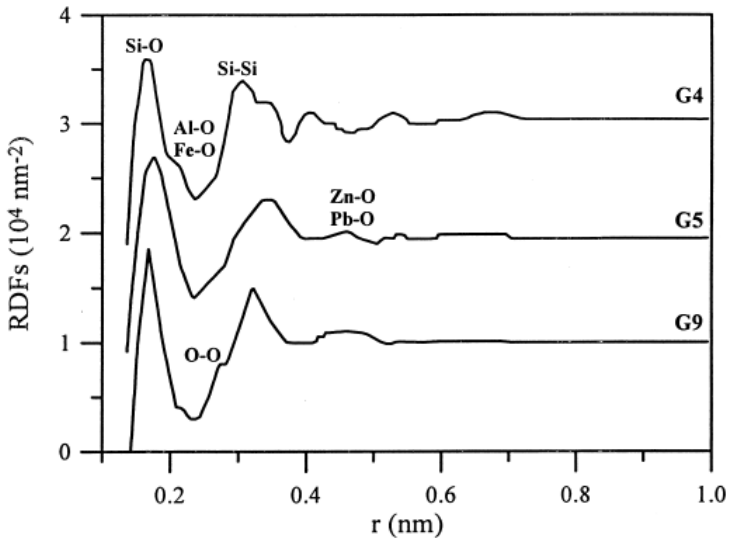

Figure 5. Electronic radial distribution functions (RDFs) for G4, G5 and G9 glasses.

The comparison between the theoretical interatomic distances calculated from ionic radii (21) with the experimental distances obtained from Figure 5 are shown in Table 4. There are some differences between theoretical and calculated values due to the difficulties in ions coupling in

the vitreous network, since the glasses and glass-ceramic are multicomponent with eight major formed oxides. Furthermore, some of these ions, like Pb^{2+}, have a high polarizability and distort the silicate network explained the differences observed.

Table 4. Theoretical and experimental interatomic distances from G4, G5 and G9 glasses.

	r (nm)			
	THEORETICAL	EXPERIMENTAL		
		G4	G5	G9
Si-O	0.16	0.16	0.17	0.17
O-O	0.26	---	---	0.27
Si-Si	0.32	0.30	0.31	0.32
Al-O	0.18	0.18	---	---
Fe^{3+}-O tetrahedral	0.18	0.18	---	---
Fe^{2+}-O octahedral	0.21	0.18	---	0.21
Zn-O	0.21	---	0.43	0.43
Pb-O	0.21	---	0.43	0.43

4. CONCLUSIONS

Mössbauer spectroscopy has determined that both Fe^{+3} and Fe^{+2} are present in the vitreous network. Fe^{+3} is in tetrahedral coordination and Fe^{2+} in octahedral coordination. The Fe^{+3}/Fe^{+2} ratio calculated by Mössbauer spectroscopy ranged from 2.6 to 5.3 and increases as the iron oxide content in the glass decreases. Fe^{2+} and Fe^{3+} quadrupole splitting values indicate that the vitreous network is more distorsioned when the iron content is greater.

The radial distribution function (RDF) of these glasses shows a simple spectrum, which indicates a network with short-range order (SRO). G4 glass shows a greater long-range order (IRO) with a very complex spectrum for interatomic distances lower than 0.4 nm. The interatomic distances determined for Si-O and Si-Si bonds ranged from 0.16 to 0.17 nm and from 0.30 to 0.32 nm respectively. Due to the difficulty of different cations coupling in the silicate glass network, some displacements in the interatomic distances are observed.

REFERENCES

1. C.R. Kurkjian, J.Non-Cryst. Solids 3, 157 (1970).
2. C.R. Kurkjian and E.A. Sigety, Phys.Chem.Glasses 9, 73 (1968).
3. J.P. Gosselin, U. Shimony, L. Grodzins and A.R. Cooper, Phys.Chem.Glasses 8, 56 (1967).
4. M.F. Tarangin and J.C. Eisenstein, J.Non-Cryst. Solids 3, 311 (1970).
5. C.H. Labar and P. Gielen, J.Non-Cryst. Solids 13, 107 (1973/74).
6. L. Pergamin, C.H.P. Lupis and P.A. Flinn, Metall.Trans. 3, 3093 (1972).
7. K. Hirao, T. Komastsu and N. Soga, J.Non-Cryst. Solids 40, 315 (1980).
8. M. Romero and J.Ma. Rincón, Materials Letters 31, 67 (1997).
9. M. Romero and J.Ma. Rincón, J.Eur.Cer.Soc. 18, 153 (1998).
10. C.N.J. Wagner, J.Non-Cryst. Solids 31, 1 (1978).
11. Y. Waseda, The Structure of Non-Crystalline Materials, McGraw-Hill, New York (1980).
12. C.N.J. Wagner, H. Ocken and Z. Joshi, Naturforsch 20a, 325 (1965).
13. V. Petkov, J.Appl.Cryst. 22, 387 (1989).
14. J.G. Stevens, Handbook of Mineral Data Mössbauer, Effect Data Center, University of North Carolina (1983).
15. G. Tomandl, Mössbauer effect in glasses, Glass: Science and Technology. Vol. 4B. Academic Press, New York (1990).
16. B.O. Mysen, Structure and Properties of Silicate Melts, Elsevier, Amsterdam (1988).
17. Menil, F., J.Phys.Chem.Solids. 46, 763 (1985).
18. Dyar, M.D., Am.Mineral. 70, 304 (1985).
19. Stevens, J.G., MRS Bulletin 21, 14 (1986).
20. P.S. Rogers and J. Williamson, Glass Technol. 10, 128 (1969).
21. J.M. Fernández Navarro, El Vidrio, Consejo Superior de Investigaciones Científicas (2ª edición), Madrid (1991).